Epitaxial growth of 20 nm InAs and GaAs quantum dots on GaAs through block copolymer templated SiO2 masks

ARTICLE *in* JOURNAL OF APPLIED PHYSICS · APRIL 2009

Impact Factor: 2.18 · DOI: 10.1063/1.3082494 · Source: IEEE Xplore

Epitaxial growth of 20 nm InAs and GaAs quantum dots on GaAs through block copolymer templated SiO_2 masks

Azar Alizadeh,[1,a)] David Hays,[1] Seth T. Taylor,[1] Chris Keimel,[1] Ken R. Conway,[1] Lauraine Denault,[1] Kasiraman Krishnan,[1] Vicki H. Watkins,[1] Rosalyn Neander,[1] Jay S. Brown,[2] Andreas Stintz,[2] Sanjay Krishna,[2] Marina Blumin,[3] Igor Saveliev,[3] Harry E. Ruda,[3] Edit Braunstein,[4] and Colin Jones[4]
[1]*GE Global Research, Niskayuna, New York 12309, USA*
[2]*Center for High Technology Materials, University of New Mexico, Albuquerque, New Mexico 87106, USA*
[3]*Department of Material Science, University of Toronto, Ontario M5S 3E4, Canada*
[4]*Missiles and Fire Control, Lockheed Martin, Orlando, Florida 32819, USA*

(Received 11 September 2008; accepted 15 January 2009; published online 6 March 2009)

We report on selective area growth of InAs and GaAs quantum dots (QDs) on GaAs through ~20 nm SiO_2 windows prepared by block copolymer lithography. We discuss the mechanisms of growth through these masks, highlighting the variation of the resulting morphology (dot size, spacing, uniformity, and areal density) as a function of growth parameters. We have obtained highly uniform arrays of InAs and GaAs QDs with mean diameters and areal densities of 20.6 nm and 1×10^{11} cm^{-2}, respectively. We have also investigated the optical characteristics of these QDs as a function of temperature and drawn correlations between the optical response and their crystalline quality. © *2009 American Institute of Physics*. [DOI: 10.1063/1.3082494]

I. INTRODUCTION

The tremendous potential of InGaAs/AlGaAs quantum dots (QDs) to revolutionize fields such as optoelectronics, information technology, field emission, and sensing has been long recognized.[1] In the past few years, a large number of QD-based optoelectronic devices, ranging from lasers and single photon sources,[2] photovoltaic and solar cells,[3] mid-wave and long-wave infrared detectors,[2] to quantum key distribution elements[2] have been fabricated. In the majority of these applications, the low dimensional semiconductor QDs are grown in the Stranski–Krastanow (SK) heteroepitaxial mode. SK grown QD arrays, however, often lack the desired size, composition, and interspacing uniformities, impairing the performance of optoelectronic devices. In addition to these shortcomings, other limitations are characteristics of, and inherent to, SK growth. The SK growth mode is only applicable to heteroepitaxial growth of materials with a lattice mismatch exceeding 2%.[1,4] Moreover, in SK growth mode, three-dimensional random nucleation and growth of QD "islands" are preceded by the initial two-dimensional growth of a wetting layer. For photodetectors based on such structures, carrier leakage from the QDs into the wetting layer can contribute to undesired temperature dependent currents.[5]

Several approaches have been proposed to control the size and location of epitaxially grown SK QDs.[1,6] However, in SK growth processes, wetting layers are inevitable and growth of lattice-matched nanostructures, such as GaAs/GaAs or GaAs/AlGaAs, is not feasible. Presently it appears that one of the more promising avenues for fabrication of tailored and highly confined semiconductor nanostructures is the selective area nanopatterned growth method.[7,8] This strategy involves the homo- or heteroepitaxial growth of nanostructures through patterned substrates or sacrificial patterned masks, allowing for precise control over QD size, shape, spacing, and uniformity. Nanopatterned selective area growth is compatible with most common epitaxial growth techniques including molecular beam epitaxy (MBE) and metal organic chemical vapor deposition (MOCVD). Lee *et al.*[9–11] reported on the selective area growth of 50–200 nm GaAs and InAs islands on a GaAs substrate patterned with a sacrificial SiO_2 mask. The authors used large area interferometric lithography and dry etching to generate the patterned SiO_2 sacrificial mask. Similarly, nanopatterned growth of 45–85 nm GaAs, InAs, and InGaAs nanostructure arrays using anodic Al_2O_3 sacrificial templates has been demonstrated.[12–14] Kiravittaya *et al.*[15,16] and Xu *et al.*[17,18] independently showed the self-assembly of highly uniform arrays of ~65 nm In(Ga)As QDs on GaAs substrates patterned (without a selective mask) through e-beam lithography and dry etching.

Patterned growth of ultradense arrays of highly confined semiconductor nanostructures requires fabrication of templates with uniform sub-20-nm features (windows) over areas as large as whole wafers. Block copolymer self-assembly and subsequent pattern transfer into a substrate or a dielectric mask allows for the fabrication of such templates.[19] Block copolymers are composed of two or more chemically different polymer chains or blocks joined covalently. Due to chemical incompatibility between the different blocks and the connectivity constraint, block copolymers can spontaneously phase segregate into well-defined morphologies, such as lamellar, cylindrical, or spherical, providing nanometer scale contrast between the different phases. The resulting morphology, in turn, depends on the relative length and composition of the individual blocks as well as their degree of interaction.[20] In the past decade, many block copolymer thin

a)Electronic mail: alizadeh@research.ge.com.

film systems have been used as lithographic masks in various nanopatterning applications.[21–26] In particular, block copolymer lithography has allowed the fabrication of sacrificial Si_xN_y and SiO_2 dielectric masks and subsequent selective area growth of very uniform GaAs, InAs, and Si/Ge QD arrays with densities as high as $\sim 10^{11}/cm^2$.[27–29]

Highly confined uniform sized InAs/GaAs QDs produced through nanopatterning approaches are of particular interest for laser and infrared detection applications. For instance, in infrared detectors based on intersublevel transitions in QDs, this growth method presents a very unique opportunity as one can realize detectors with a very narrow spectral width that are needed in multispectral and hyperspectral imaging systems. In this paper, we report on selective area growth of InAs and GaAs QDs on GaAs through ~20 nm SiO_2 windows prepared by block copolymer lithography. The impact of substrate and growth interface on the final QD morphology (size and uniformity) will be discussed. We have used MBE and modulated MBE techniques for the growth of QDs and have characterized QD morphology, size, spacing, uniformity, and areal density as a function of different growth parameters. The mechanisms of nanopatterned growth through the SiO_2 masks are discussed as a function of growth conditions. Correlations are drawn between the optical characteristics of the QDs, as measured by photoluminescence (PL) spectroscopy at various temperatures, and their atomic and defect structures as revealed by high-resolution transmission electron microscopy (HRTEM).

II. EXPERIMENTAL SECTION

A. Fabrication and patterning of SiO_2 templates

We have used polystyrene-*b*-polymethyl methacrylate (PS-PMMA) block copolymer lithography to produce the SiO_2 templates. The principles of PS-PMMA lithography are described in great detail in reports by Russell and co-workers.[19,22] A brief description of the self-assembly process on GaAs and subsequent etching is presented here. A 20–30 nm thick SiO_2 layer is deposited on a semi-insulating or *n*+ doped GaAs (001) substrate using plasma enhanced chemical vapor deposition at 270 °C. A 5–7 nm brush layer of a random PS-*r*-PMMA copolymer with a molecular weight, M_w, of 8.9 kg/mol, polydispersity, M_w/M_n, of 1.47 and PS content of 59.4% (Polymer Source Inc.) is grafted to the SiO_2 surface. This treatment neutralizes the interactions of the surface with each of the blocks of the block copolymer so that perpendicular orientation of the PMMA cylinders can be achieved.[30] Next $a \sim 25$ nm film of PS-PMMA with a M_w of 67.1 kg/mol, $M_w/M_n = 1.09$, and PS content of 68.7% (Polymer Source Inc.) is spin coated on the surface and annealed at 170 °C for ~2 h. The PMMA cylinders are then removed upon blanket exposure to UV light (245 nm) and subsequent wash with acetic acid. This process is similar to photolithography where UV light is exposed onto a photosensitive resist through a patterned mask, causing a solubility change. The nanoporous PS film is used as an etch mask for pattern transfer into the 20–30 nm SiO_2 layer employing CHF_3 reactive ion etching in a capacitively coupled plasma reactor.

B. MBE and modulated MBE growth of QDs

MBE using As_2 and elemental group III sources were used for the growth of InAs and GaAs nanostructures. To remove potential surface contamination and assure good crystal quality at the growth interface, the templates were subjected to a precleaning protocol consisting of (1) wet etch with $HF:H_2O$ (1:400) for 15 s, de-ionized water, and $NH_4OH:H_2O_2$ (1:30) for 20 s; (2) vacuum bake at 550 °C for 30 min, followed by a final bake at 650 °C under As flux for 10 min. InAs and GaAs islands of varying thicknesses were then deposited by MBE onto the SiO_2-patterned substrates. Growth parameters such as In, Ga, and As flux rates, temperature and growth time were varied to optimize the morphology and uniformity of the QD arrays. Additional improvement in QD size and density uniformity was obtained using time modulation of the Ga, In, and As fluxes during MBE. We will refer to this process as modulated MBE.

A series of single layer SK QD arrays were also grown for comparison purposes. Subsequent to growth of a 1 μm thick GaAs buffer layer at 590 °C, 1 nm thick $In_{0.15}Ga_{0.85}As$ and 1.67 ML (monolayer) of InAs islands were grown at 470 °C. The details of MBE growth are described elsewhere.[31]

C. Morphology and optoelectronic characterization of QDs

Field emission scanning electron microscopy (SEM) and scanning force microscopy were used to characterize the nanopatterned templates and the QD arrays. Conventional and high-resolution phase contrast imaging and energy dispersive spectroscopy (EDS) studies were performed on ion-milled cross sections, using a 200 keV field-emission transmission electron microscope (FEI G2 Tecnai TF20). PL studies were carried out in the temperature range of 7.5 to 280 K. A Ti sapphire laser (800 nm) with an incident power density of ~30 W/cm^2 was used as an excitation source. A liquid nitrogen cooled InSb detector was used to characterize the PL signal from the QD arrays.

III. RESULTS AND DISCUSSION

A. Nanopatterned growth of InAs and GaAs QDs

Figure 1(a) shows a typical top view SEM image of the SiO_2 mask produced with block copolymer lithography. A highly uniform array of holes with an average diameter of 21 ± 2 nm and spacing (center to center) of 38 ± 3 nm is obtained. As mentioned previously, a pregrowth cleaning protocol is required to assure high crystal quality at the growth interface. Figure 1(b) shows a top view SEM image of the substrate/growth interface subsequent to the pregrowth cleaning and removal of the SiO_2 template with hydrofluoric acid (HF). As a result of pregrowth cleaning, etch pits with faceted perimeters are developed in the GaAs substrate. These crystallographic etch pits are 5–10 nm deep. As shown later, the etch pits have a profound impact on the nucleation and formation of the InAs or GaAs QDs during the patterned growth process. It should be noted that the lack of pattern transfer in several regions of Fig. 1(b) is due to nonunifor-

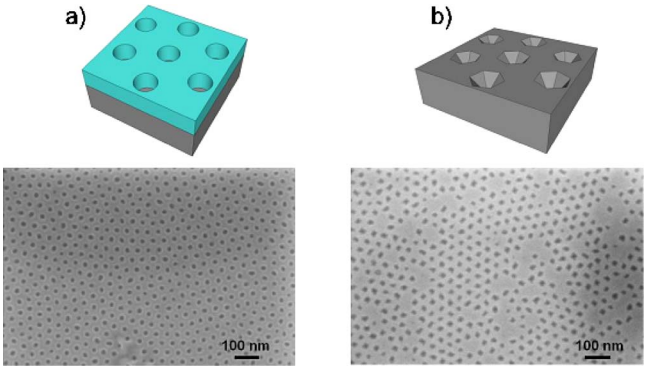

FIG. 1. (Color online) (a) Schematic and top view SEM image of a GaAs substrate with SiO2 mask patterned through block copolymer lithography. (b) Schematic and top view SEM image of the substrate subsequent to pregrowth cleaning and mask removal.

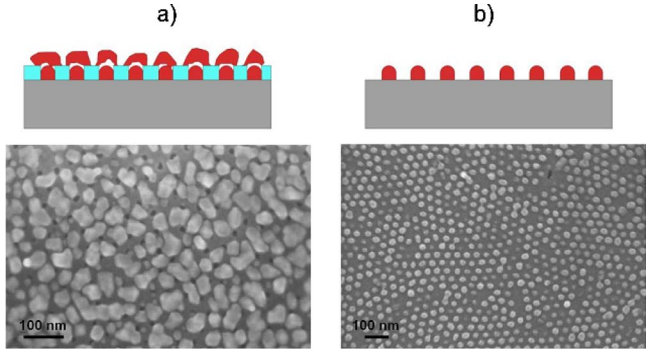

FIG. 3. (Color online) Schematic and top view SEM images of (a) nonselective growth with deposition on the mask and inside the pores before mask removal and (b) after mask removal.

mities of the block copolymer pattern itself. In the current study, self-assembly of the block copolymer films was performed at 170 °C for a relatively short period of time (<2 h). A more extended annealing of block copolymer films often results in a much more uniform and less defective patterns. However, in this study, we did not focus on improving the long-range order of the patterns.

Several MBE growth parameters were investigated for achieving area-selective epitaxy of uniform size InAs QD arrays. To find the optimal temperature range, we developed an experimental methodology to provide MBE deposition on the substrate with a temperature gradient, as schematically shown in Fig. 2(a): A strip of GaAs wafer with SiO_2 mask contacting with the heated subholder only at the two ends provides a nonuniform temperature distribution across the substrate with a minimum at the center. The temperature of the sample was measured by calibrated optical pyrometry. SEM images of the nanopatterned grown InAs QDs, without mask removal, at several temperature regions are shown in Figs. 2(b)–2(e). Arsenic to indium flux ratio, in equivalent

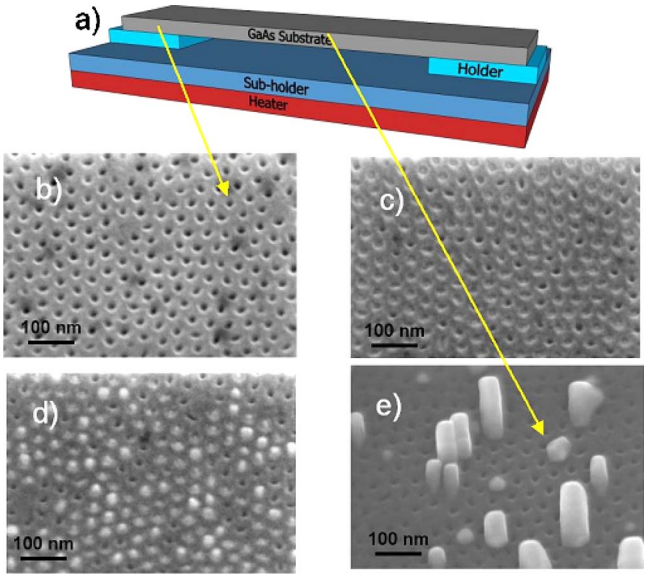

FIG. 2. (Color online) (a) Schematic of MBE sample holder with variable temperature gradient. Top view SEM images at various growth temperatures: (b) $T>580$ °C (no deposition), (c) $T\sim570$ °C (selective growth), (d) $T\sim530$ °C (selective growth), and (e) $T<530$ °C (nonselective growth).

beam pressure, and growth time were equal to ~15 and 6 min, respectively. At elevated temperatures (>580 °C), the probability of InAs nucleation on the SiO_2 mask and inside the ~20 nm GaAs windows is very low. Accordingly, the majority of the holes remain empty [Fig. 2(b)]. On the other hand, in the low temperature region, the pore filling is very nonuniform and nucleation of InAs on the mask occurs. As a result, nonselective growth and even nonuniform arrays of nanostructures are obtained [Fig. 2(e)]. We will return to this growth regime later. In the intermediate temperature region, ~530–570 °C, the pore filling is very uniform and nucleation of InAs on the SiO_2 mask is negligible [Figs. 2(c) and 2(d)]. This observation is in agreement with previous studies by Lee *et al.*[10,11] who found the sticking coefficient of In atoms to SiO_2 to be close to zero under similar growth conditions. It should be noted that Lee *et al.*, in their theoretical and experimental studies, used SiO_2 masks with larger patterned windows (50–200 nm). This, in turn, indicates that the conditions for selective MBE growth of InAs QDs are template feature size independent. Selective area growth through masks with ~10 nm features will be a subject of future investigations. In the intermediate temperature range, there are subtle differences in the mechanism of InAs QD growth. At higher temperatures, ~570 °C, In adatoms can readily desorb from the SiO_2 surface. As a result, InAs QD formation is mainly dictated by the incoming flux through the ~20 nm windows. In contrast, at ~530 °C, In adatoms diffuse for much longer times on the SiO_2 surface and may be trapped in the pores. Thus, in the latter case, most of the incoming In atoms contribute to QD formation, as opposed to the former case, where significant desorption takes place. Clear evidence for this is shown in Figs. 2(c) and 2(d), where under identical flux conditions, QDs grown through diffusion (or migration) assisted processes fill up a larger portion of the pores.

Nanopatterned growth of uniform InAs QD arrays can also be achieved through nonselective area processes at $T<530$ °C. In this case, the sticking of In atoms to the mask is non-negligible. Therefore, simultaneous nucleation of InAs occurs on the SiO_2 mask and inside the pores. Figure 3(a) and 3(b) illustrate an example of such situation before and after mask removal, respectively. As it can be seen in Fig. 3(b), despite the nonselective nature of the growth, pore filling and pore uniformity are excellent. Similar results have

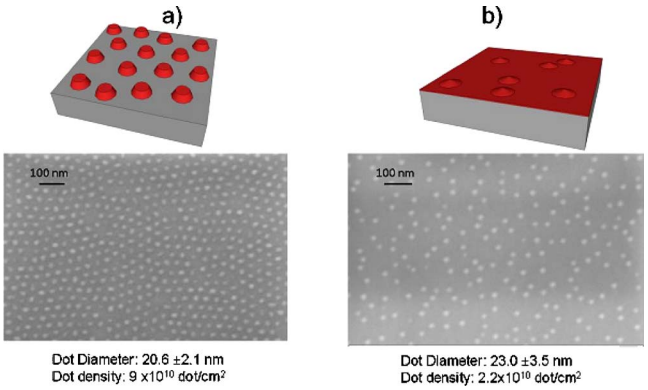

FIG. 4. (Color online) Schematic and top view SEM images of (a) nanopatterned grown InAs QDs subsequent to template removal: Diameter= 20.6 ± 2.1 nm, density=and (b) SK QDs: Diameter= 23.0 ± 3.5 . nm, density=

been previously observed on patterned growth of InAs nanostructures using anodic alumina masks.[14] Modulated MBE experiments have been very useful in achieving selective area growth of InAs even at lower temperatures. In modulated MBE, the In and As shutters in the growth chamber are opened at different time intervals, such that In atoms are allowed to diffuse over extended distances with minimum As adatoms present to prevent their capture.

In Figs. 4(a) and 4(b) the morphologies of nanopatterned and SK grown InAs QDs are compared. The MBE conditions (T=535 °C, As to In flux ratio=10, growth rate =0.1 ML/s, growth time=387 s) were chosen to achieve negligible growth of InAs on the SiO_2 mask, i.e., selective area growth. Subsequent to mask removal with HF, a very uniform array of QDs with regular spacing is obtained [Fig. 4(a)]. SK growth conditions (see experimental condition) were chosen to achieve similar size dots [Fig. 4(b)]. In order to estimate the average dot dimensions, spacing and corresponding standard deviations, several SEM images, exceeding 1000 dots, were analyzed using standard image analysis tools. The corresponding values are reported in the caption of Fig. 4. The random nature of the nucleation process in the SK case is responsible for larger variation in size and spacing uniformities. The block copolymer patterned masks alleviate this problem considerably. The density of the nanopatterned QDs in this case is $\sim 9\times 10^{10}/\mathrm{cm}^2$. These results are in agreement with other block copolymer nanopatterned growth data reports on Si/Ge and GaAs nanostructures.[27–29] Fabrication of templates with smaller size openings is possible through the use of lower molecular weight block copolymers,[19] which would enable nanopatterned growth of ultrahigh density QD arrays while maintaining outstanding size uniformity.

The lateral dimensions and spacing of the QDs perfectly mirror the morphology of the SiO_2 template, while their height mainly depends on the mask height and growth conditions. The height of SK QDs is governed by growth conditions and the balance between substrate/dot surface energies and strain fields. Typically, the height of SK QDs is between 5 and 8 nm.[1,2] In contrast, with the nanopatterned growth approach, QD heterostructures with tailored higher aspect ratios and geometries can be obtained. The average heights of the nanopatterned grown InAs QDs in Figs. 4(a) and 4(b) are 12 and 6 nm, respectively. To ensure QD height uniformity, the desired dot height in the template should not exceed the height of the template. We have observed a large dispersion in both dot height and shape when attempting to grow dots whose heights were larger than the template thickness. This may be due to the fact that growth is no longer inhibited by the confined SiO_2 window once the surface of the SiO_2 is breached. At this point, growth is expected to accelerate significantly perhaps promoting different growth regimes. That is, the growth is no longer selective.

Inspection of QD cross sections by HRTEM and EDS reveals that InAs dot formation is usually initiated at the base of etch pits formed below the GaAs substrate surface. We indicated earlier that these etch pits are a result of the pregrowth cleaning process [see Fig. 1(b)]. In Fig. 5(a), Moiré fringes in the TEM image result from interference of overlapping lattice planes of different spacing, suggesting the presence of InAs QDs in the etched pits of the GaAs. The inset chemical line profile, achieved by stepping a focused electron probe across the QD/substrate interface and acquiring energy dispersive x-ray spectra at periodic intervals,

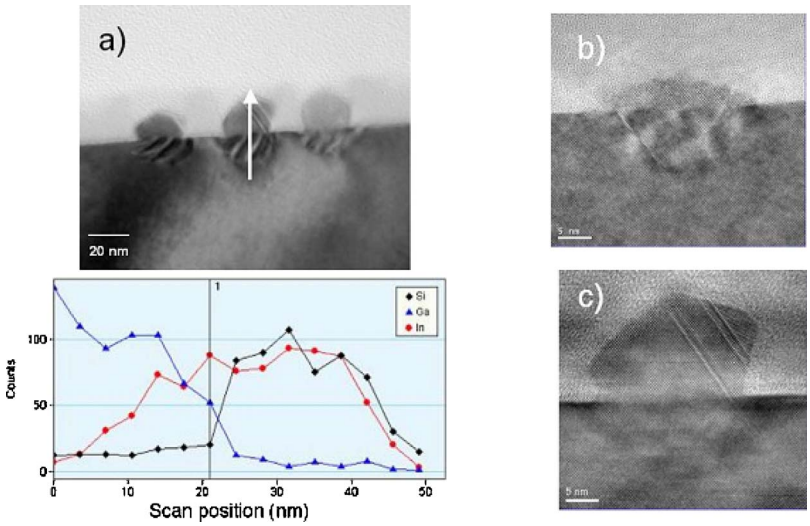

FIG. 5. (Color online) (a) TEM and EDS line profile of nanopatterned grown QDs revealing subsurface nucleation of InAs. (White arrow in image indicates scan direction for line profile). HRTEM images of InAs QDs grown for (b) 387 and (c) 774 s, reveal the presence of twinning defects.

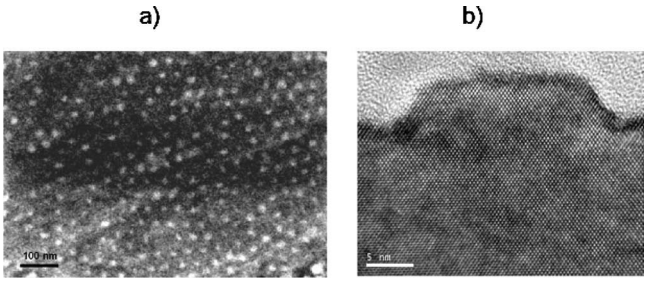

FIG. 6. Homoepitaxial nanopatterned growth of GaAs QDs on GaAs: (a) top view SEM and (b) HRTEM images.

shows mixing of the In and Ga below the substrate surface. HRTEM images of two InAs QDs grown at 535 °C for 387 and 774 s are shown in Figs. 5(b) and 5(c), respectively. The HRTEM images once again provide evidence for pit formation followed by InAs QD filling. Surface faceting of the larger InAs QD structure is observed in Fig. 5(c). In both cases, QDs contain twinned regions near the growth edges. We speculate that these regions may form as part of a deformation mechanism to accommodate local stresses arising during growth in a confined volume. More detailed studies will be required to understand this mechanism and to mitigate its effects on QD structure and performance. Several factors, including lattice mismatch between GaAs and InAs, the presence of the SiO_2 mask, preferential nucleation inside the etch pits, preferential nucleation on non (001) crystallographic planes, or preferred nucleation on a concave (as opposed to a planar) surface, may contribute to local stress development and thus defect formation, during the growth process. We are currently investigating the growth of InAs QDs on patterned GaAs substrates, in the absence of sacrificial SiO_2 masks, to better understand the nature and mechanisms of selective area growth.

Homoepitaxial nanopatterned growth of 15 nm GaAs QDs through ~20 nm SiO_2 windows was carried out at 646 °C and growth rate of=0.1 μm/h. In order to maximize pore filling and dot size uniformity a modulated MBE approach was used where Ga and As shutters were opened and closed, nonsimultaneously, for short periods of time during 114 cycles. In each cycle, the Ga shutter was opened first for 10 s, then all the shutters were closed for 10 s before opening the As shutter for another 10 s. An additional 10 s were allowed between two consecutive cycles. Under these MBE conditions, GaAs nucleates on the SiO_2 mask and inside the windows. Figures 6(a) and 6(b) show top view SEM and cross-sectional HRTEM images of the resulting GaAs QDs after mask removal. A highly uniform array of dots with similar areal density as for InAs is obtained. Due to the lattice match between the QD and the underlying substrate, the growth interfaces and QDs are defect-free as revealed in the HRTEM image. Homoepitaxial area-selective growth of GaAs QDs on block copolymer patterned GaAs substrates, using MOCVD tools, has been previously demonstrated.[27,29] The nanopatterned MBE growth work presented here, which relies on migration-assisted processes, yields almost identical results with respect to areal density, dot size, and spacing uniformities. MBE area-selective growth of GaAs on nanopatterned substrates is definitely feasible, as demonstrated by Lee *et al.*[9] Optimization of MBE growth conditions to achieve selective area nanopatterned homoepitaxy will be the subject of future investigations.

B. Optical properties of InAs QDs

Figure 7(a) shows the PL characteristics of the nanopatterned and SK InAs QDs at 7.5 K, respectively. The growth conditions are identical to those reported in Figs. 4(a) and 4(b). Broad PL emission intensity curves peaking around 1600 nm are observed in both cases. A lower PL intensity is obtained for the nanopatterned QDs. The broad luminescence for SK QDs is attributed to fluctuations in their size distribution. On the other hand, for the nanopatterned QDs, the spectral broadening and a lower PL signal may reflect fluctuations in strain and alloy composition within the large illuminated area. As explained earlier, factors such as nucleation and growth inside etch pits contribute to strain and defect development in the nanopatterned dots. The etch pits are developed during the pregrowth cleaning process and can vary in depth and geometry. Consequently, the nanopatterned

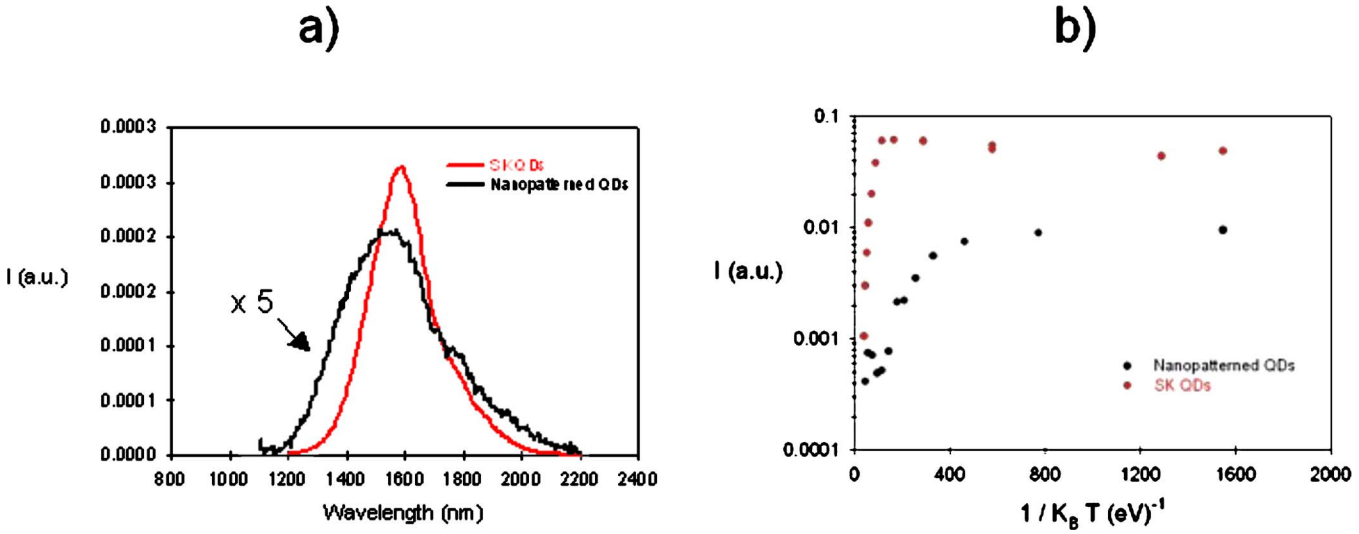

FIG. 7. (Color online) (a) PL curves of nanopatterned and SK QDs at 7.5 K. In the case of nanopatterned QDs, the PL intensity has been multiplied by 5. (b) Integrated PL intensities of nanopatterned and SK QDs as a function of temperature.

dots growing inside these etch pits may experience different strain fields. It should also be noted that the dots are not capped and an optimized capping layer during the epitaxial growth is known to reduce the inhomogeneous broadening of the PL spectrum.

PL experiments were conducted in the temperature range of 7.5–250 K. A slight redshift in PL peak position is observed as the sample temperature is increased. The observed PL spectrum is assumed to represent recombination from a distribution of QD sizes, where the high-energy part of the distribution comes from smaller QDs. As the temperature is increased, the smaller QDs are preferentially thermalized, and this gives rise to a redshift in the observed (ensemble) PL spectrum. For each QD array, the decrease in PL emission with the increase in temperature is expected. This reduction may be attributed to exciton dissociation or to competing thermally activated processes. Electrons and holes in the QDs can be reemitted to the GaAs barrier layer prior to their radiative recombination in the QD.[32] For SK QDs, PL emission is observed in the entire temperature range (4–300 K). In contrast, the PL signal in nanopatterned QDs is suppressed for temperatures above 100 K. The temperature dependence of the integrated PL intensity was analyzed as a function of the inverse of temperature for both QD arrays [see Fig. 7(b)]. A single activation energy barrier model is used to fit the data, where the temperature dependence of the PL intensity is expressed as $I(T)=I_0/\{1+C\exp(-E_a/K_BT)\}$.[33] The corresponding activation energies, E_a, for the nanopatterned and SK QDs are equal to 12 and 92 meV, respectively. Lower activation energies in patterned grown InGaAs nanostructures as compared to SK has been previously observed through cathodoluminescence studies.[34] Suppression of PL at elevated temperature and low activation energy values in patterned QDs can be explained in terms of the presence of interface and defect states. Such states may be associated with nonideal growth interfaces, however, the exact nature of the electronic states in these nanopatterned dots is not known.

In summary, we have demonstrated the nanopatterned growth of ~20 nm InAs and GaAs QD on GaAs substrates patterned with sacrificial SiO_2 masks. Block copolymer lithographic tools have allowed for fabrication of highly dense arrays of small size holes in the SiO_2 masks. We have also shown a strong correlation between the optoelectronic performance, as evidenced by PL, and the internal structures of the QDs. The presence of nonideal growth interfaces as well as the SiO_2 mask may contribute to local stress development and thus defect formation during the growth process. Further studies will be required to reduce defect formation in these nanostructures.

ACKNOWLEDGMENTS

This work was supported by the GE/Lockheed Martin Shared Vision program. We are very thankful to M. L. Blohm, S. Vitkavage, J. Grande, and O. Boomhower for support and helpful discussions.

[1] D. Bimberg, M. Grunmann, and N. N. Ledentsov, *Quantum Dot Heterostructures* (Wiley, New York, 1999).
[2] P. Bhattacharya, D. Bimberg, and Y. Arakawa, Special Issue of Proc. IEEE **95**, 1718 (2007).
[3] A. Luque and S. Hegedus, *Handbook of Photovoltaic Science and Engineering* (Wiley, New York, 2003).
[4] P. R. Berger, K. Chang, P. Bhattacharya, J. Singh, and K. K. Bajaj, Appl. Phys. Lett. **53**, 684 (1988).
[5] R. Heitz, A. Kalburge, Q. Xie, M. Grundmann, P. Chen, A. Huffmann, A. Madhukar, and D. Bimberg, Phys. Rev. B **57**, 9050 (1998).
[6] S. Krishna, K. Linder, and P. Bhattacharya, J. Appl. Phys. **86**, 4691 (1999).
[7] K. Tachibana, T. Someya, I. Satomi, and Y. Arakawa, Appl. Phys. Lett. **76**, 3212 (2000).
[8] A. Alizadeh, P. Sharma, S. Ganti, S. F. LeBoeuf, and L. Tsakalakos, J. Appl. Phys. **95**, 8199 (2004).
[9] S. C. Lee, K. J. Malloy, and S. R. J. Brueck, J. Appl. Phys. **90**, 4163 (2001).
[10] S. C. Lee, A. Stintz, and S. R. J. Brueck, J. Appl. Phys. **91**, 3282 (2002).
[11] S. C. Lee, R. Dawson, S. R. J. Brueck, and A. Stintz, J. Appl. Phys. **96**, 4586 (2004).
[12] X. Mei, D. Kim, H. E. Ruda, and Q. X. Guo, Appl. Phys. Lett. **81**, 361 (2002).
[13] X. Mei, M. Blumin, M. Sun, D. Kim, Z. H. Wu, H. E. Ruda, and Q. X. Guo, Appl. Phys. Lett. **82**, 967 (2003).
[14] X. Mei, M. Blumin, D. Kim, Z. Wu, and H. E. Ruda, J. Cryst. Growth **251**, 253 (2003).
[15] S. Kiravittaya, H. Heidemeyer, and O. G. Schmidt, Physica E (Amsterdam) **23**, 253 (2004).
[16] S. Kiravittaya, A. Ratelli, and O. G. Schmidt, Appl. Phys. Lett. **87**, 243112 (2005).
[17] J. Liang, H. Luo, R. Beresford, and J. Xu, Appl. Phys. Lett. **85**, 5974 (2004).
[18] W. Guo, R. S. Guico, R. Beresford, and J. M. Xu, J. Cryst. Growth **287**, 509 (2006).
[19] C. J. Hawker and T. P. Russell, MRS Bull. **30**, 952 (2005).
[20] F. S. Bates and G. H. Fredrickson, Phys. Today **52**(2), 32 (1999).
[21] C. Harrison, D. H. Adamson, Z. Cheng, J. M. Sebastian, S. Sethuraman, D. A. Huse, R. A. Register, and P. M. Chaikin, Science **290**, 1558 (2000).
[22] T. Thurn-Albrecht, J. Schotter, G. A. Kastle, N. Embly, T. Shibauchi, L. Krusin-Elbaum, K. Guarini, C. T. Black, M. T. Tuominen, and T. P. Russell, Science **290**, 2126 (2000).
[23] K. W. Guarini and C. T. Black, J. Vac. Sci. Technol. B **20**, 2788 (2002).
[24] J. Y. Cheng, C. A. Ross, E. L. Thomas, H. I. Smith, and G. J. Vansco, Appl. Phys. Lett. **81**, 3657 (2002).
[25] R. A. Segalman, H. Yokoyama, and E. J. Kramer, Adv. Mater. (Weinhem, Ger.) **13**, 1152 (2001).
[26] R. D. Peters, M. Xiao, Q. Wang, J. J. de Pablo, and P. F. Nealey, J. Vac. Sci. Technol. B **18**, 3530 (2000).
[27] R. P. Li, P. D. Dapkus, M. E. Thompson, W. G. Jeong, C. Harrison, P. M. Chaikin, R. A. Register, and D. H. Adamson, Appl. Phys. Lett. **76**, 1689 (2000).
[28] Z. M. Zhao, T. S. Yoon, W. Feng, B. Y. Li, J. H. Kim, J. Liu, O. Hulko, Y. H. Xie, H. M. Kim, K. B. Kim, K. L. Wong, C. Ratsch, R. Catflisch, D. Y. Ryu, and T. P. Russell, Thin Solid Films **508**, 195 (2006).
[29] J. H. Park, A. A. Khanekar, S. M. Park, L. J. Mawst, T. F. Kuech, and P. F. Nealey, J. Cryst. Growth **297**, 283 (2006).
[30] D. Y. Ryu, K. Shin, E. Drokenmuller, C. J. Hawker, and T. P. Russell, Science **308**, 236 (2005).
[31] A. Stintz, G. T. Liu, A. L. Gray, R. Spillers, S. M. Delgado, and K. J. Malloy, J. Vac. Sci. Technol. B **18**, 1496 (2000).
[32] D. H. Rich, Y. Tang, A. Konkar, P. Chen, and A. Madhukar, J. Appl. Phys. **84**, 6337 (1998).
[33] G. Bacher, H. Schweizer, J. Kovac, A. Forchel, H. Nickel, W. Schlapp, and R. Losh, Phys. Rev. B **43**, 9312 (1991).
[34] Q. X. Guo, X. Mei, H. Ogawa, and H. E. Ruda, Jpn. J. Appl. Phys., Part 1 **41**, 7297 (2002).